Supplementary Materials for "Origin of Positive/Negative Effects on Pressure-Dependent Thermal Conductivity: The Role of Bond Strength and Anharmonicity"

Fang Lyu,[1] Wei Cao,[2, a)] Han-Pu Liang,[3] Tan Peng,[2] Yue Hou,[2] Xiaolu Zhu,[2] Ling Miao,[4] Ziyu Wang,[1, 2, b)] Rui Xiong,[1, c)] and Jing Shi[1]

[1)] *School of Physics and Technology, Wuhan University, Wuhan 430072, China.*

[2)] *The Institute of Technological Science, Wuhan University, Wuhan 430072, China.*

[3)] *Beijing Computational Science Research Center, Beijing 100193, China.*

[4)] *School of Optical and Electronic Information, Huazhong University of Science and Technology, Wuhan 430074, China.*

[a)]Electronic mail: Corresponding author.wei_cao@whu.edu.cn

[b)]Electronic mail: Corresponding author.zywang@whu.edu.cn

[c)]Electronic mail: Corresponding author.xiongrui@whu.edu.cn

I. METHODOLOGY AND COMPUTATIONAL DETAILS

TABLE S1. The lattice constants **a** and **b** (Å), mass ratio and coefficients (eV/$\AA^2$) of the second order polynomial fitting to the atomic potential energy for XSe (X = Be, Mg, Ca) of $F\bar{4}3m$ and $Fm\bar{3}m$ phases.

	XSe	l	mass ratio	$2nd$
$F\bar{4}3m$	BeSe	**a** , **b** = 5.182	8.762	11.550
	MgSe	**a** , **b** = 5.992	3.249	9.480
	CaSe	**a** , **b** = 6.595	1.970	8.240
$Fm\bar{3}m$	BeSe	**a** , **b** =4.922	8.762	0.920
	MgSe	**a** , **b** = 5.504	3.249	2.150
	CaSe	**a** , **b** = 5.965	1.970	2.300

The bond strength and anharmonicity are assessed using the Regular Residual Analysis method[1,2], based on the standard Taylor series expansion function $f(x)$

$$f(x) = f(0) + \frac{1}{1!}f^{'}(0)x + \frac{1}{2!}f^{''}(0)x^2 + \frac{1}{3!}f^{'''}(0)x^3 + \frac{1}{4!}f^{''''}(0)x^4 + ..., \tag{1}$$

where x represents a small perturbation around the equilibrium position, set at 0, along the chemical bond. This function also signifies the atomic potential energy. In practical calculations,

$$F(x) = ax^2 - bx^3 + cx^4 + Ox^5, \tag{2}$$

Here, a, $-b$, and c represent the coefficients of the second-, third-, and fourth-order terms, respectively. The term Ox^5 represents the sum of higher-order terms, describing the anharmonicity of the potential energy. The regular residual e, defined as the difference between the calculated observed values $F(x)_i$ and the predicted values $F(x)$, is determined as follows:

$$e = F(x)_i - F(x). \tag{3}$$

Here, we calculated the atomic potential energy with respect to displacement of Group IIA selenides XSe in both $F\bar{4}3m$ and $Fm\bar{3}m$ phases. There only one single bond changes in the

conventional cell of each configuration, and keeping all other bonds unchanged. Then, the coefficient of the second-order fitting indicate the bond strength as shown in Table S1 and Figure S1-S2.

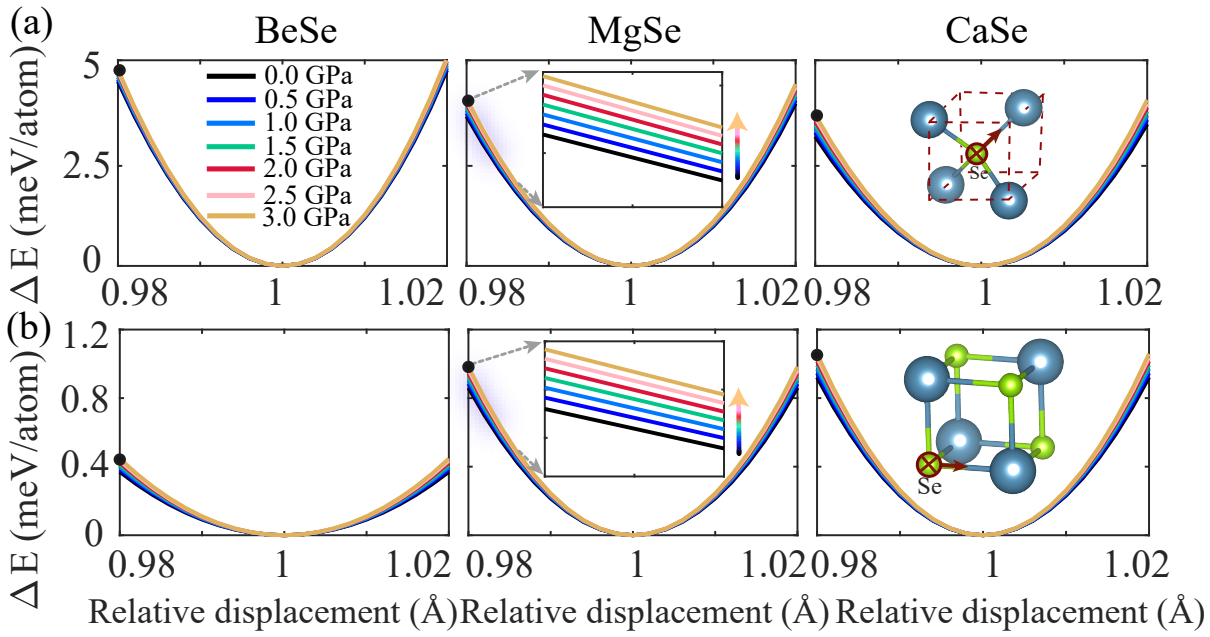

Fig. S1. The potential energy curves as a function of Se atomic displacement along the bond in (a) $F\bar{4}3m$ and (b) $Fm\bar{3}m$ phases.

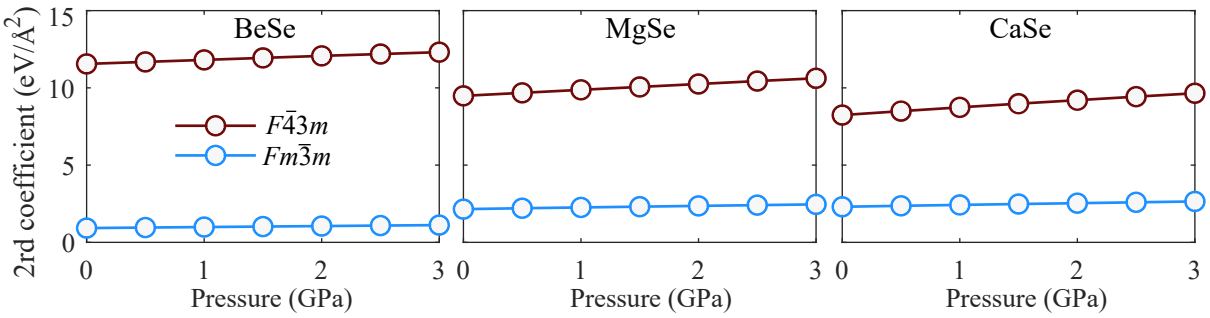

Fig. S2. The coefficients of second order polynomial fitting with respect to the pressure of XSe (X = Be, Mg, Ca) in $F\bar{4}3m$ and $Fm\bar{3}m$ phases, respectively.

Further, we present the elastic properties to evaluate the strength of interatomic bonding and lattice anharmonicity as illustrated in Figure S3. The bonding characteristics analysis using a Crystal Orbital Hamiltonian Population (COHP) by the LOBSTER package[3], which given the bonding and anti-bonding character of the DOS at each energy.

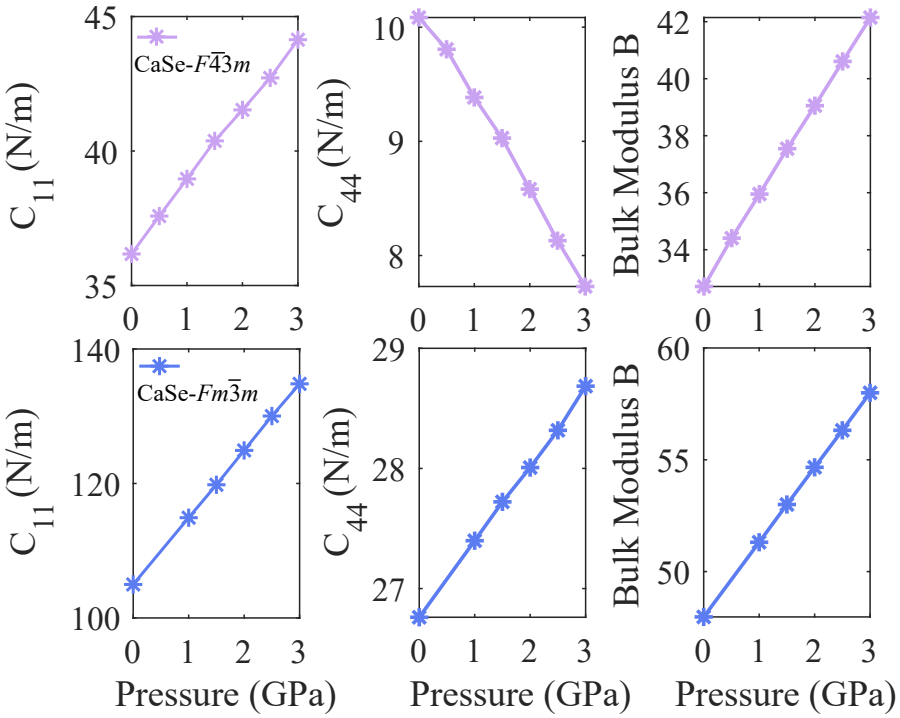

Fig. S3. The elastic properties as a function of pressure for CaSe in (a) $F\bar{4}3m$, and (b) $Fm\bar{3}m$ phases.

II. CONVERGENCE TEST OF LATTICE THERMAL CONDUCTIVITY

The convergence test including the scalebroad parameter and the nearest neighbor with different q-point of thermal conductivity as shown in Figure S4. It can be seen the thermal conductivity decreases under pressure. The $15\times15\times15$ q-points grid, 10th nearest neighbors, and scalebroad = 0.1 smearing parameter are sufficient for achieving convergence.

Details of phonon-phonon interactions, including group velocity, phase space, and phonon scattering rates in the $F\bar{4}3m$ CaSe structure are shown in Figure S5 - S7. It is found that, with the increase of pressure, the group velocity increases at 3 THz, which is consistent with the large slope of phonon branches. The phase space is almost unchanged, and the phonon scattering is significant at low frequency, consistent with thermal conductivity results.

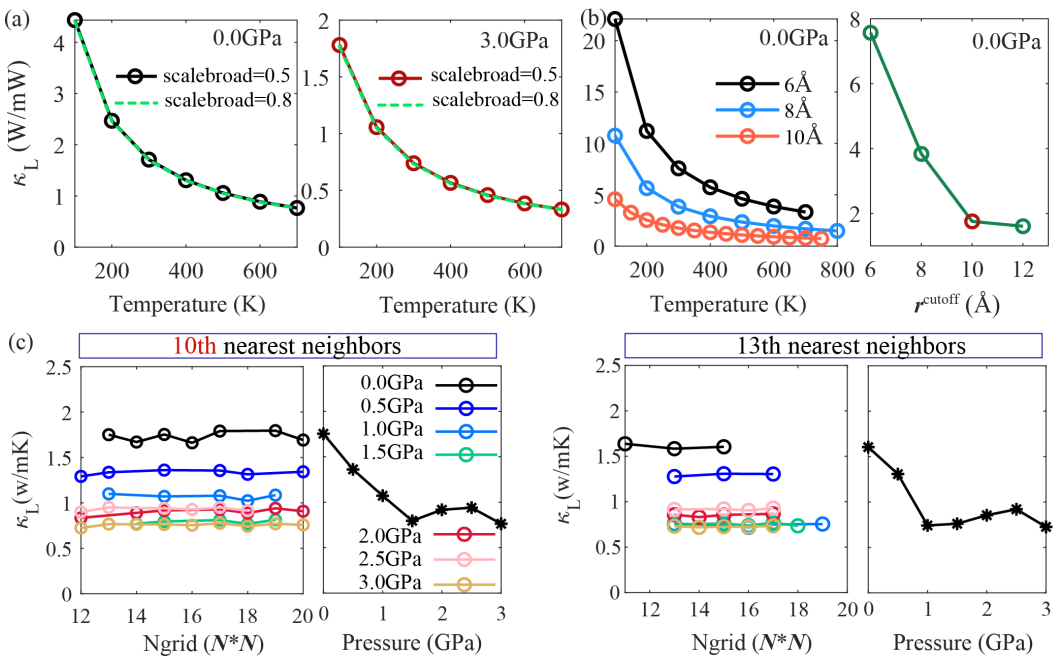

Fig. S4. The lattice thermal conductivity κ_L test of $F\bar{4}3m$ CaSe configuration, (a) at different scalebroad values of 0.0 GPa and 3.0 GPa, (b) at different cutoff radius of r^{cutoff} with respect to the temperature under 0.0 GPa, (c) at different nearest neighbors of third-order IFCS with 300K.

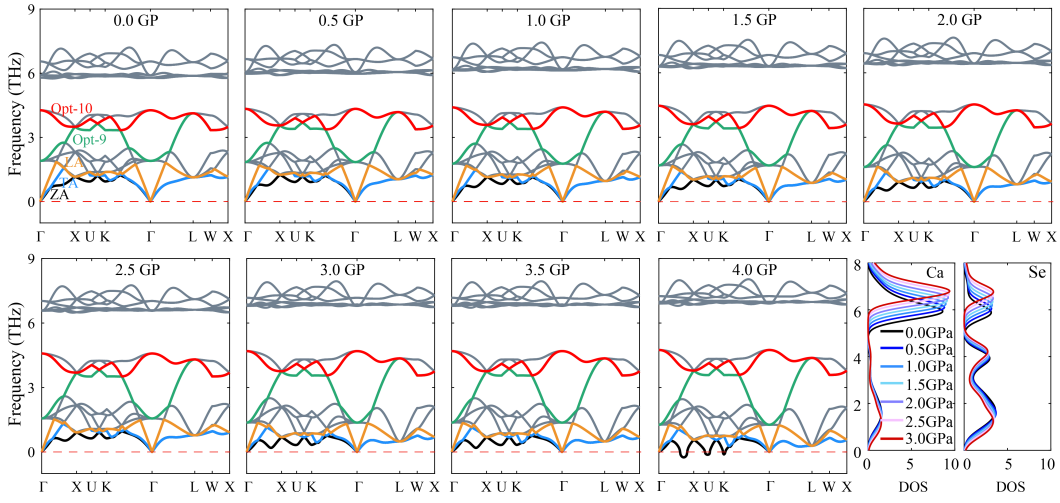

Fig. S5. Phonon spectra as well as densities of state (DOS) for $F\bar{4}3m$ CaSe configuration.

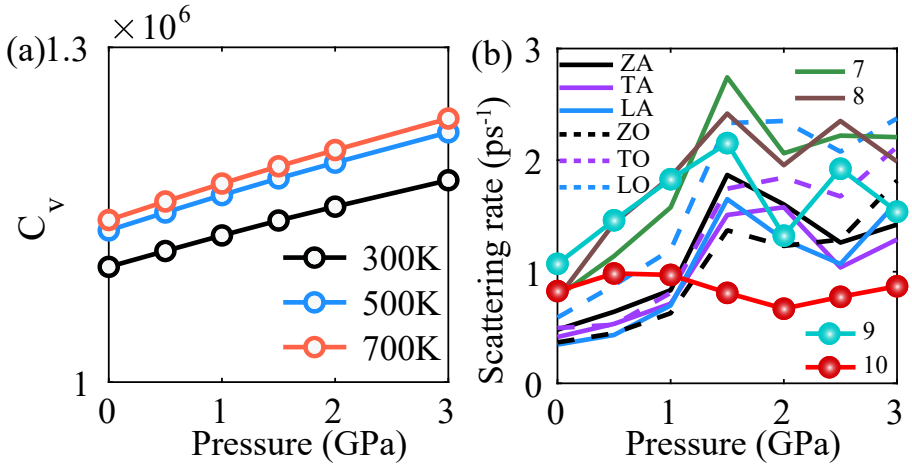

Fig. S6. The (a) heat capacity C_V versus pressure at 300 K, 500 K, and 700 K. (b) Scattering rate contribution versus pressure at 300 K for each phonon branch of $F\bar{4}3m$ CaSe configuration.

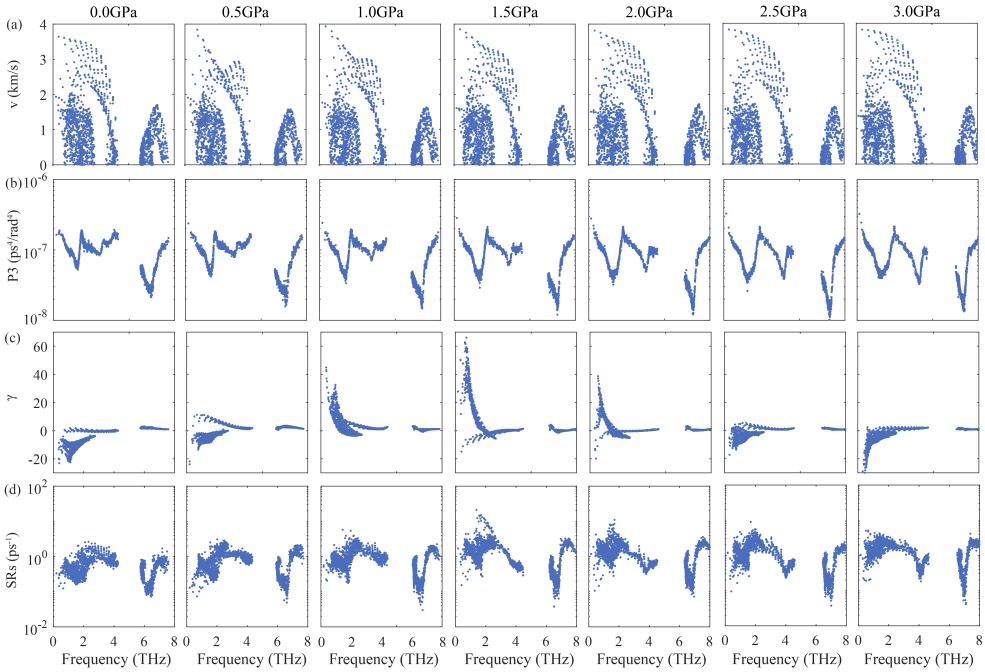

Fig. S7. (a) The phonon group velocity v, (b) phase space $P3$, (c) Grüneisen parameter γ, and (d) scattering rates SRs with respectively various pressures and frequency at 300 K in $F\bar{4}3m$ CaSe configuration.

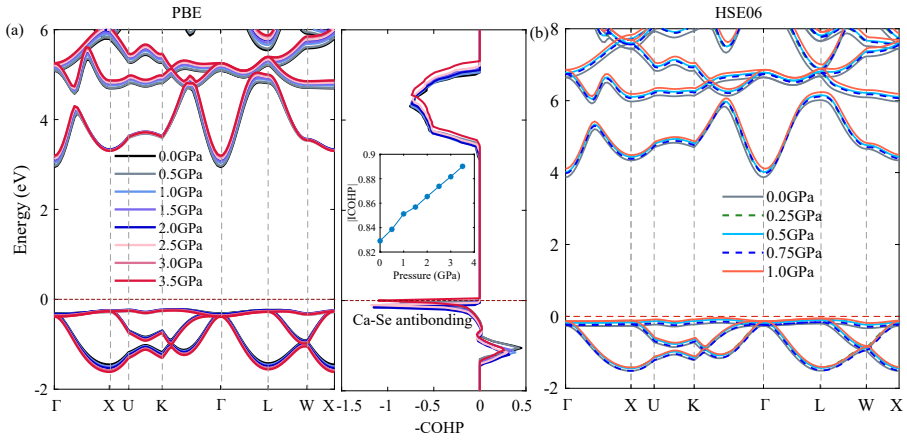

Fig. S8. (a) The DPT (PBE) hybrid functional band structure and the crystal orbital Hamilton population (COHP) under pressures, (b) HSE06 hybrid functional band structure with various pressures in $F\bar{4}3m$ CaSe configuration.

III. ELECTRON TRANSPORT COEFFICIENT

The different carrier scattering rate based on the Fermi golden rule from initial $\psi_{n\mathbf{k}}$ to final state $\psi_{m\mathbf{k+q}}$ can be written as

$$\widetilde{\tau}^{-1}_{n\mathbf{k}\to m\mathbf{k+q}} = \frac{2\pi}{\hbar} \mid g_{nm}(\mathbf{k},\mathbf{q}) \mid^2 \delta(\epsilon_{n\mathbf{k}} - \epsilon_{m\mathbf{k+q}}), \tag{4}$$

in which n and m are the sign of the energy level, $\mathbf{k}$ and $\mathbf{k}+\mathbf{q}$ denote the coordinates of reciprocal space, $\epsilon_{n\mathbf{k}}$ is the energy state $\psi_{n\mathbf{k}}$, and $g_{nm}(\mathbf{k},\mathbf{q})$ is the electron-phonon scattering matrix element from initial state $\psi_{n\mathbf{k}}$ into final state $\psi_{m\mathbf{k+q}}$. Finally, the rational carrier relaxation time τ can be calculated,

$$\frac{1}{\tau} = \frac{1}{\tau^{\mathrm{ADP}}} + \frac{1}{\tau^{\mathrm{IMP}}} + \frac{1}{\tau^{\mathrm{POP}}}, \tag{5}$$

where ADP, IMP, and POP are the scattering rates of the anisotropic acoustic deformation potential, the ionized impurity, and the polar optical phonon, respectively.

The acoustic deformation potential matrix element is given by

$$g^{\mathrm{ADP}}(\mathbf{k},\mathbf{q}) = \left[\frac{k_B T \epsilon_d^2}{B}\right]^{\frac{1}{2}} < \psi_{\mathbf{k+q}} \mid \psi_{\mathbf{k}} >, \tag{6}$$

where k_B is the Boltzmann constant, T is temperature, ϵ_d is the volume-deformation potential at the valence band maximum, B is the bulk modulus. The ionized impurity scattering

rate can be written as

$$g^{\mathrm{IMP}}(\mathbf{k},\mathbf{q}) = \left[\frac{e^2 n_{ii}}{\epsilon_s^2}\right] \frac{< \psi_{\mathbf{k+q}} \mid \psi_{\mathbf{k}} >}{\mid \mathbf{q} \mid^2 + \beta^2}, \tag{7}$$

where e is the electron charge, β is the inverse screening length calculated from the density of states, n_{ii} is the concentration of ionized impurities. The above parameters can be calculated by first principles. Since the exact ionized impurity concentration cannot be determined, the concentration is set equal to the number of free carriers. The polar optical phonon scattering rate is given by

$$g^{\mathrm{POP}}(\mathbf{k},\mathbf{q}) = \left[\frac{\hbar\omega_{po}}{2}(\frac{1}{\epsilon_\infty} - \frac{1}{\epsilon_s})\right] \frac{< \psi_{\mathbf{k+q}} \mid \psi_{\mathbf{k}} >}{\mid \mathbf{q} \mid}, \tag{8}$$

where $\hbar$ is the reduced Planck constant, ω_{po} is an effective optical phonon frequency, ϵ_∞ is the high-frequency dielectric constant, ϵ_s is the static dielectric constant.

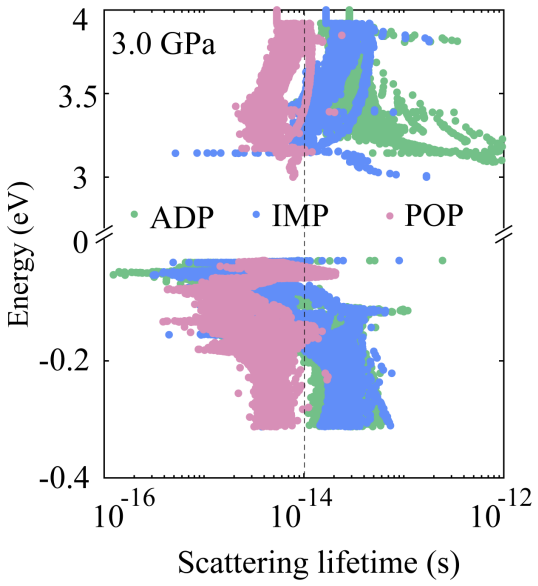

Fig. S9. Carrier scattering lifetime at the ADP, IMP, and POP scattering mechanisms near the conduction- and valence-band edges as a function of energy under 3.0 GPa of $F\bar{4}3m$ CaSe configuration.

REFERENCES

[1]S.-Y. Yue, X. Zhang, G. Qin, S. R. Phillpot, and M. Hu, Phys. Rev. B **95**, 195203 (2017).

[2]S.-Y. Yue, G. Qin, X. Zhang, X. Sheng, G. Su, and M. Hu, Phys. Rev. B **95**, 085207 (2017).

[3]M. S, D. VL, T. AL, and D. R, J. Comput. Chem. **37**, 1030 (2016).

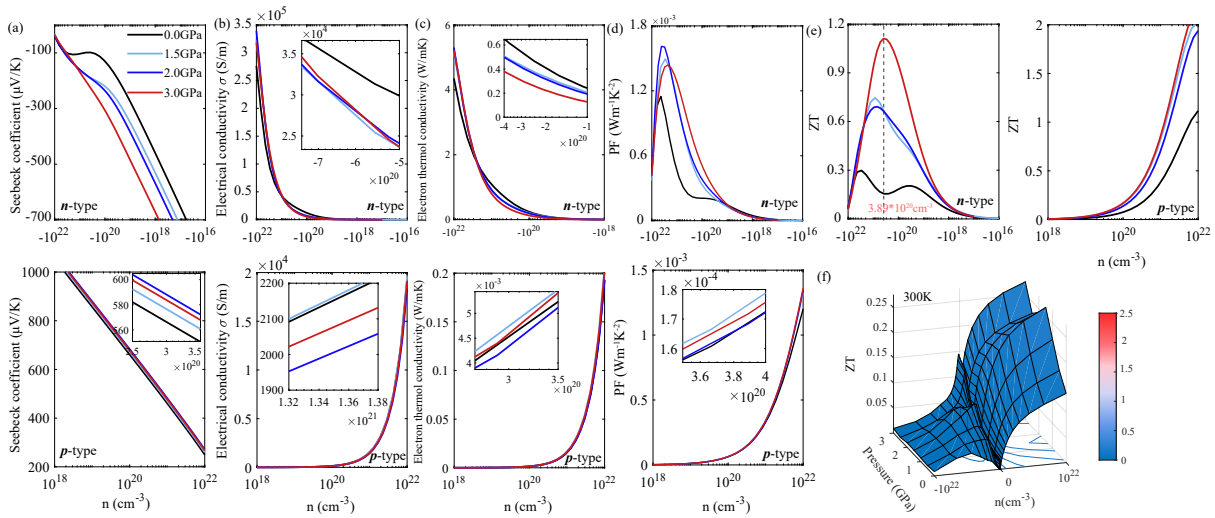

Fig. S10. Calculated electronic transport coefficients (a) Seebeck coefficient S, (b) electrical conductivity σ, (c) Electron thermal conductivity κ_e, (d) power-factor PF, and (e) figure of merit ZT of $F\bar{4}3m$ CaSe as a function of carrier concentrations with respectively various pressures at 800 K. (f) The figure of merit ZT for n-type and p-type doping versus the carrier concentration and pressure of $F\bar{4}3m$ CaSe at 300 K.